

---

# Conjugation with $^{111}\text{In}$ -DTPA-Poly(Ethylene Glycol) Improves Imaging of Anti-EGF Receptor Antibody C225

Xiaoxia Wen, Qing-Ping Wu, Shi Ke, Lee Ellis, Chusilp Charnsangavej, Abraham S. Delpassand, Sidney Wallace, and Chun Li

*Division of Diagnostic Imaging and Department of Surgical Oncology, University of Texas M.D. Anderson Cancer Center, Houston, Texas*

---

Significant liver uptake often limits the clinical application of radiolabeled antibodies in radioimmunodetection. The purpose of this study was to evaluate the  $\gamma$ -imaging properties of an antiepidermal growth factor receptor (EGFR) antibody, C225, conjugated with heterofunctional poly(ethylene glycol) (PEG) with 1 terminus of the polymer attached to a radiometal chelator, diethylenetriaminepentaacetic acid (DTPA). **Methods:** Two preparations of PEG-modified C225, one with 20% and the other with 60% amine substitution, were labeled with  $^{111}\text{In}$ . The conjugates,  $^{111}\text{In}$ -DTPA-PEG-C225, were injected intravenously into nude mice with EGFR-positive A431 tumors. For comparison, C225 directly labeled with  $^{111}\text{In}$  was also injected. In a competitive study, mice with A431 tumors were pretreated intravenously with 100-fold excess of native C225, followed by an injection of  $^{111}\text{In}$ -DTPA-PEG-C225 30 min or 20 h later. In addition,  $^{111}\text{In}$ -DTPA-PEG-C225 was injected into mice with EGFR-positive MDA-MB-468 tumors and EGFR-negative MDA-MB-435 tumors. Images were acquired at 5 min and at 2, 6, 24, and 48 h after injection of the radiotracers. Regions of interest (ROIs) were drawn on the computer images around the whole body, liver, muscle, and tumor. The counts per pixel in the tumor and normal tissues were calculated. At 48 h, the mice were killed and dissected. Blood, liver, muscle, and tumor samples were removed and the radioactivity of each sample was measured. **Results:** In A431 tumor xenografts, the tumor uptake of C225 modified with PEG was not significantly different than the uptake of unmodified  $^{111}\text{In}$ -DTPA-C225. Uptake in the liver, however, was reduced by 38%–45%, and the reduction increased with increasing degree of PEG substitution. Tumors of A431 and MDA-MB-468 xenografts were clearly visualized with  $^{111}\text{In}$ -DTPA-PEG-C225, whereas tumors of the MDA-MB-435 xenograft, which expresses low levels of EGFR, were not as readily visible. The tumor-to-blood ratios of  $^{111}\text{In}$ -DTPA-PEG-C225 in A431 and MDA-MB-468 xenografts were about 3 fold higher than in MDA-MB-435 xenografts. Blocking EGFR by pretreatment with native C225 significantly reduced the uptake of  $^{111}\text{In}$ -DTPA-PEG-C225 in the liver. The tumor-to-blood ratios in mice with A431 tumors were decreased 2.5–2.7 fold after pretreatment with a large excess of C225. Similar results were

obtained with MDA-MB-468 tumor xenografts. In contrast, the tumor-to-blood ratios in mice with MDA-MB-435 tumor xenografts were not significantly different in C225-pretreated mice than in nonpretreated mice. **Conclusion:** These findings indicate that  $^{111}\text{In}$ -DTPA-PEG-C225 selectively localized to the tumors expressing high levels of EGFR. PEG-modification of C225 significantly reduced its liver uptake, resulting in improved visualization of EGFR-positive tumors. Using PEG as a linker between the monoclonal antibody and metal chelator is a useful strategy to optimize the imaging characteristics of antibody-based scintigraphic agents.

**Key Words:** epidermal growth factor receptor; monoclonal antibody C225;  $^{111}\text{In}$ ; imaging

**J Nucl Med 2001; 42:1530–1537**

---

**E**pidermal growth factor receptor (EGFR) is a transmembrane glycoprotein with an intracellular tyrosine kinase domain. EGFR is frequently overexpressed on the cells of many solid tumors (1–3). The high level of expression of this receptor is found to be associated with tumor proliferation and poor prognosis. EGFR, therefore, is an excellent target for antitumor diagnosis and therapy (1). C225 is a human–mouse chimeric monoclonal antibody that targets EGFR. It selectively binds to the external domain of the receptor with affinity comparable with the natural ligand ( $K_d = 1 \text{ nmol/L}$ ) and competes with EGF binding (4,5). C225 has been shown to inhibit EGFR tyrosine kinase activity and proliferation of a variety of cultured malignant epithelial cell lines that express high levels of EGFR (6–8). It also has shown significant antitumor efficacy against human breast, colon, prostate, and cervical cancer xenografts. C225 is currently undergoing a series of phase II clinical trials in which it is combined with doxorubicin for advanced prostate cancer, with cisplatin for advanced head, neck, and lung cancer, and with paclitaxel for breast cancer (4,9–11).

The effectiveness of a therapeutic intervention targeted to EGFR will depend on its ability to detect and characterize EGFR-expressing lesions throughout the body. To achieve

---

Received Dec. 4, 2000; revision accepted May 29, 2001.

For correspondence or reprints contact: Chun Li, PhD, Division of Diagnostic Imaging, Box 59, University of Texas M.D. Anderson Cancer Center, 1515 Holcombe Blvd., Houston, TX 77030.

the best results for C225-directed immunotherapy, it is necessary to assess the presence of EGFR before treatment, to confirm *in vivo* tumor targeting by the antibody, and to evaluate the therapeutic response. The gold standard for the evaluation of EGFR status is immunohistologic examinations. This method, however, is limited by its invasiveness, the heterogeneity of tumors, and the inaccessibility of some tumors, particularly metastases, to biopsy procedures. A noninvasive imaging method using radiopharmaceuticals targeted to EGFR would be useful in characterizing the level of EGFR expression at the tumor sites and appropriately selecting patients for therapy directed against EGFR.

C225 attached to the radiometal chelator diethylenetriaminepentaacetic acid (DTPA) and labeled with  $^{111}\text{In}$  has been shown to localize specifically in tumors that overexpress EGFR (12). Phase I studies showed that  $^{111}\text{In}$ -DTPA-C225 was able to image squamous cell lung carcinomas expressing high levels of EGFR and metastases >1 cm in diameter. However, considerable hepatic radioactivity was seen as a result of nonspecific uptake (13). In a recent study, another anti-EGFR monoclonal antibody, mAb 528, was labeled with  $^{111}\text{In}$  through DTPA (14). Although radiolabeled mAb 528 localized in EGFR-positive MDA-MB-468 human tumor xenografts more efficiently than radiolabeled EGF peptide, both compounds had high uptake in the liver and kidney. The accumulation of radiolabeled anti-EGFR antibodies in a healthy liver and kidney could limit their clinical usefulness for the detection of primary tumors as well as metastases in the chest and abdominal area. To overcome this drawback and optimize the imaging properties of C225, we introduced flexible, linear poly(ethylene glycol) (PEG) molecules into C225 to reduce nonspecific interaction. In a previous study, we developed a simple, 1-step synthesis of DTPA-PEG-conjugated C225 from a key PEG intermediate that has metal chelator DTPA attached to the termini of the polymer chain. We also have shown that DTPA-PEG-C225 and  $^{111}\text{In}$ -labeled DTPA-PEG-C225 retained the biologic activity of C225 with reduced nonspecific binding (15). The objective of this study was to investigate the imaging properties of  $^{111}\text{In}$ -DTPA-PEG-C225 in EGFR-positive and EGFR-negative human tumor xenografts and to compare the results with those obtained with  $^{111}\text{In}$ -DTPA-C225.

## MATERIALS AND METHODS

### Materials

C225 was provided by ImClone Systems Inc. (New York, NY). DTPA-PEG-C225 was synthesized according to a previously described method (15). A key intermediate, DTPA-PEG-acetylthioacetate, was first prepared from *N*-succinimidyl-*s*-acetylthioacetate (Sigma Chemicals, St. Louis, MO) and DTPA-PEG-NH<sub>2</sub>, which in turn was obtained by reacting t-BocNH-PEG-NH<sub>2</sub> (Shearwater Polymers, Inc., Huntsville, AL) with DTPA-dianhydride (Sigma Chemicals). Immediately before the reaction with maleimide-activated C225 (*N*- $\gamma$ -maleimidobutyryloxysuccinimide ester; Sigma Chemicals), the protecting group in DTPA-PEG-acetylthioacetate

was removed by hydroxylamine (Sigma Chemicals) to give DTPA-PEG-SH. The product was purified by gel filtration chromatography using the Sephacryl S-200 HR column (Amersham Pharmacia Biotech, Piscataway, NJ). Two preparations of DTPA-PEG-C225 were used in the imaging study. In the 1:10 DTPA-PEG-C225 conjugate (where 1:10 denotes the molar ratio of C225 to maleimide), approximately 20% of the lysine amine groups in the antibody were activated. In the 1:30 DTPA-PEG-C225 conjugate, approximately 60% of the amines were derived. The degree of derivation was estimated based on analysis of unreacted amino groups in the modified antibodies using TNBS assay (picrylsulfonic acid; Sigma Chemicals). DTPA-C225 was prepared by reacting C225 directly with DTPA-dianhydride as described previously (16). The conjugate was purified by gel filtration on a PD-10 column (Amersham Pharmacia Biotech).

### Radiolabeling

Generally, 40  $\mu\text{g}$  of each antibody conjugate in 100  $\mu\text{L}$  phosphate-buffered saline (PBS) was incubated with 13.0–14.8 MBq (350–400  $\mu\text{Ci}$ )  $^{111}\text{InCl}_3$  in 20  $\mu\text{L}$  1 mol/L sodium acetate buffer, pH 5.5 (Dupont–New England Nuclear, Boston, MA), at room temperature for 15 min. The resulting radiopharmaceutical was purified from free  $^{111}\text{In}$  by gel filtration on a PD-10 column using PBS as the eluent. Fractions of 0.5 mL were collected. The radioactivity of each fraction was measured by a radioisotope calibrator (CRC-12R; Capintec Instruments, Ramsey, NJ). The protein content in each fraction was determined using a protein assay kit (Bio-Rad Laboratories, Hercules, CA) according to the manufacturer's instructions. The fractions containing the protein were combined. The radiochemical purities of 1:10  $^{111}\text{In}$ -DTPA-PEG-C225, 1:30  $^{111}\text{In}$ -DTPA-PEG-C225, and  $^{111}\text{In}$ -DTPA-C225, determined by gel permeation chromatography, were 97%, 99%, and 99%, respectively.

### Cell Lines

Human breast adenocarcinoma cell lines MDA-MB-468, MDA-MB-435, and human vulvar squamous carcinoma cell line A431 were maintained in 1:1 (v/v) Dulbecco's modified Eagle's medium/Ham's F-12 mixture supplemented with 10% fetal bovine serum (Gibco Laboratories, Grand Island, NY) at 37°C in 5% CO<sub>2</sub>/95% air. Both MDA-MB-468 and A431 cell lines express high levels of EGFR (12). To determine the EGFR expression in MDA-MB-435 cells, 80  $\mu\text{g}$  total protein from cell lysates of each sample were resolved by 10% sodium dodecylsulfate polyacrylamide gel electrophoresis. The proteins were electroblotted onto Immobilon-NC HAHY nitrocellulose membrane (Millipore Corporation, Bedford, MA). The membrane was blocked in 10% nonfat dry milk for 2 h at room temperature, incubated with monoclonal anti-EGFR antibody (Sigma Chemicals) at 4°C overnight, and treated with horseradish peroxidase-conjugated goat antimouse secondary antibodies (Jackson Immuno Research Laboratories, West Grove, PA) for 1 h at room temperature. A signal was detected using the ECL Western blotting detection system (Amersham Pharmacia Biotech).

### Whole-Body Scintigraphy and Dissection Analysis

Female BALB/c mice with a nu/nu background were subcutaneously injected with A431, MDA-MB-468, or MDA-MB-435 cells ( $1 \times 10^7$ /site) in the chest and the right hind limb. When the xenografts reached 8–10 mm in diameter, the mice were divided into groups of 3 each. The mice were anesthetized by an intraperitoneal injection of sodium pentobarbital (35 mg/kg), then admin-

istered with 10  $\mu\text{g}$  1:10  $^{111}\text{In}$ -DTPA-PEG-C225, 1:30  $^{111}\text{In}$ -DTPA-PEG-C225, or 1.85–3.7 MBq (50–100  $\mu\text{Ci}$ )  $^{111}\text{In}$ -DTPA-C225 through the tail vein. An Orbiter gamma camera (Siemens Gammasonics, Des Plaines, IL), equipped with a medium-energy collimator and Elscint Apex SPX-1 software (Siemens), was used for the  $\gamma$ -imaging. The mice were placed prone on the camera's pinhole collimator. The images were acquired in a  $128 \times 128$  matrix for 15 min, immediately after injection and at 2, 6, 24, and 48 h after injection of the radiotracer. Regions of interest (ROIs) were drawn on the computer images around the whole body, liver, muscle, and tumor. The counts per pixel in the tumor and normal tissues were calculated.

At 48 h after injection, the mice were killed and dissected. Blood samples were obtained by cardiac puncture, and samples of the liver, muscle, and tumor were removed from each animal. Radioactivity of each sample was measured with the Cobra Auto-gamma Counter (Packard, Downers Grove, IL). The percentage of the injected dose per gram of tissue (%ID/g tissue) was calculated for each sample.

### Competition with Unlabeled C225

In separate experiments, native C225 at a dose of 1 mg per mouse was injected intravenously 30 min or 20 h before injection of 10  $\mu\text{g}$  1:30  $^{111}\text{In}$ -DTPA-PEG-C225 (1.85 MBq [50  $\mu\text{Ci}$ ]) into mice with A431, MDA-MB-468, or MDA-MB-435 tumors. The mice were scanned at 24 and 48 h after injection of the radiotracer. The mice were killed at 48 h, and tumor, liver, muscle, and blood samples were collected for the quantification of radioactivity by a  $\gamma$ -counter.

### Statistical Analysis

Statistical comparisons were calculated using a Student *t* test ( $P < 0.05$ ).

## RESULTS

### Tumor Imaging with $^{111}\text{In}$ -DTPA-C225 and $^{111}\text{In}$ -DTPA-PEG-C225

Whole-body  $\gamma$ -scintigrams of mice bearing A431 tumors obtained at different intervals after intravenous injection of  $^{111}\text{In}$ -DTPA-C225, 1:10  $^{111}\text{In}$ -DTPA-PEG-C225, or 1:30  $^{111}\text{In}$ -DTPA-PEG-C225 are presented in Figures 1, 2, and 3, respectively. Immediately after injection of each radiotracer, images showed the highest activity in the central location, which is attributable to the cardiac blood pool, the liver, and the spleen. Although activity in the liver of mice injected with  $^{111}\text{In}$ -DTPA-C225 dominated the images at 24 and 48 h (Fig. 1), significant reduction of radioactivity in the liver was seen with PEG-modified C225 conjugates, particularly at 24 and 48 h (Figs. 2 and 3). Tumors at both inoculation sites (hind limb and chest) were visualized 24 h after injection with all 3 C225 radiotracers. However, only tumors in mice injected with 1:30  $^{111}\text{In}$ -DTPA-PEG-C225 were clearly seen 48 h after injection (Fig. 3).

These observations were confirmed by ROI image quantification. The tumor radioactivity relative to whole-body counts per pixel for all 3 radiotracers increased over time; this increase plateaued at 24 h (data not shown). Figure 4 presents the tumor-to-liver ratios per pixel as a function of time. PEG-modified C225 conjugates had significantly

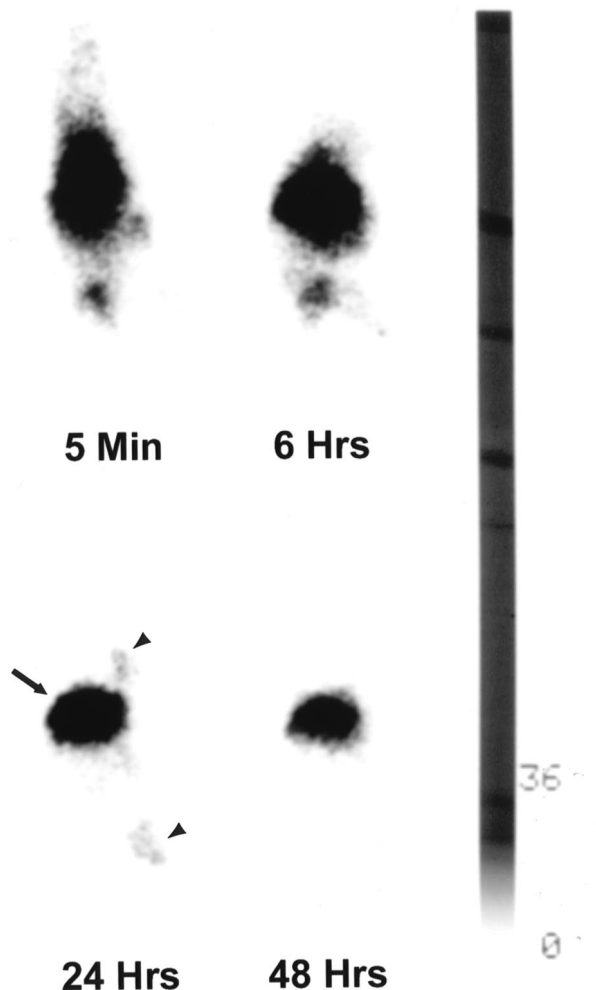


**FIGURE 1.** Sequential  $\gamma$ -images of mouse injected with  $^{111}\text{In}$ -DTPA-C225. Mouse, which had A431 tumors (arrowheads) in chest and right hind limb, was administered 10  $\mu\text{g}$   $^{111}\text{In}$ -DTPA-C225 through tail vein. Whole-body images were obtained 5 min and 6, 24, and 48 h after injection. Radioactivity was predominantly in liver (arrow) at 24 and 48 h after injection. Anterior views of mouse placed prone on camera's pinhole collimator, with head pointing to top.

higher tumor-to-liver ratios than C225 without PEG modification at each analyzable time point ( $P < 0.05$ ), and the values increased with time until 24 h after the radiotracer injection. Dissection analysis performed 48 h after injection of the radiotracers showed that the liver uptake was markedly reduced in the mice that received PEG-modified radiotracer, from  $46.9 \pm 2.5$  %ID/g for DTPA-C225 to  $27.0 \pm 3.0$  %ID/g and  $25.5 \pm 2.0$  %ID/g for 1:10 and 1:30  $^{111}\text{In}$ -DTPA-PEG-C225, respectively. The radioactivity of PEG-ylated C225 in blood was increased as a result of decreased liver uptake. The tumor uptake was unchanged with the lower degree of PEG modification ( $11.2 \pm 0.8$  %ID/g for 1:10  $^{111}\text{In}$ -DTPA-PEG-C225 vs.  $11.0 \pm 1.0$  %ID/g for  $^{111}\text{In}$ -DTPA-C225) or decreased only moderately with the

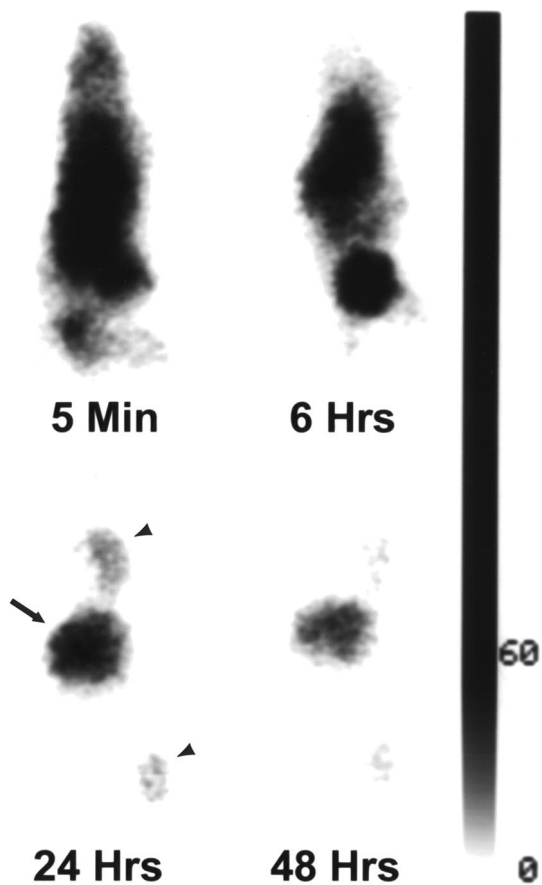


**FIGURE 2.** Sequential  $\gamma$ -images of mouse injected intravenously with  $10\ \mu\text{g}$  1:10  $^{111}\text{In}$ -DTPA-PEG-C225. Tumors are seen in 24-h postinjection image (arrowheads). Radioactivity in liver (arrow) is markedly lower than in images in Figure 1. Anterior views of mouse placed prone on camera's pinhole collimator, with head pointing to top.

higher degree of PEG modification ( $8.7 \pm 1.8\ \%\text{ID/g}$  for 1:30  $^{111}\text{In}$ -DTPA-PEG-C225) (Table 1).

#### Effect of C225 Pretreatment on Imaging and Distribution

Mice with A431 tumors were pretreated with 1 mg native C225 20 h before intravenous injection of 1:30  $^{111}\text{In}$ -DTPA-PEG-C225.  $\gamma$ -Scintigrams of the mice taken at 6 and 24 h after the radiotracer injection showed markedly reduced liver uptake of  $^{111}\text{In}$ -DTPA-PEG-C225 in both groups. Although suppression of tumor activity was seen in mice injected with C225 20 h before radiotracer injection (Fig. 5), this effect was not obvious in scintigrams of mice given C225 30 min before injection of the radiotracer (data not shown).

Dissection analysis performed 48 h after injection of 1:30  $^{111}\text{In}$ -DTPA-PEG-C225 showed that pretreatment with C225 significantly reduced the tumor-to-blood ratio ( $P < 0.05$ ) (Table 1). Tumor-to-muscle ratio also was reduced, albeit to a lesser degree. Pretreatment with C225 signifi-

cantly reduced liver uptake of 1:30  $^{111}\text{In}$ -DTPA-PEG-C225 ( $P < 0.005$  at 20-h interval;  $P < 0.05$  at 30-min interval). As a result, blood-pool activity was significantly elevated. It is interesting that pretreatment with C225 only caused a moderate decrease in tumor uptake of the radiotracer when the interval between the administration of C225 and 1:30  $^{111}\text{In}$ -DTPA-PEG-C225 was 20 h. At a shorter interval (30 min) between the delivery of the 2 agents, the uptake of  $^{111}\text{In}$ -DTPA-PEG-C225 in the tumor was actually significantly increased ( $P < 0.05$ ; Table 1).

#### Imaging of Tumors as Function of EGFR Expression

To show that  $^{111}\text{In}$ -DTPA-PEG-C225 can localize specifically in tumors that overexpress EGFR, we used human tumor xenografts expressing different levels of EGFR in the  $\gamma$ -imaging study. Western analysis of A431, MDA-MB-468, and MDA-MB-435 confirmed that both A431 and MDA-MB-468 express high levels of EGFR, whereas MDA-MB-435 expresses negligible amounts of EGFR (data

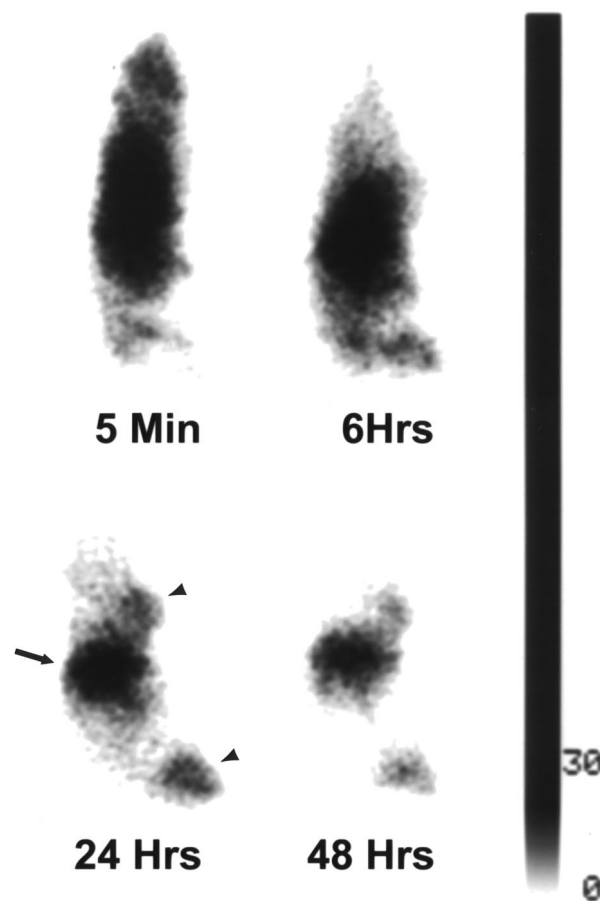


**FIGURE 3.** Sequential  $\gamma$ -images of mouse injected intravenously with  $10\ \mu\text{g}$  1:30  $^{111}\text{In}$ -DTPA-PEG-C225. Radioactivity in liver (arrow) is markedly lower than in images in Figure 1. Tumor (arrowheads) in hind limb is clearly seen at 6, 24, and 48 h after injection. Anterior views of mouse placed prone on camera's pinhole collimator, with head pointing to top.

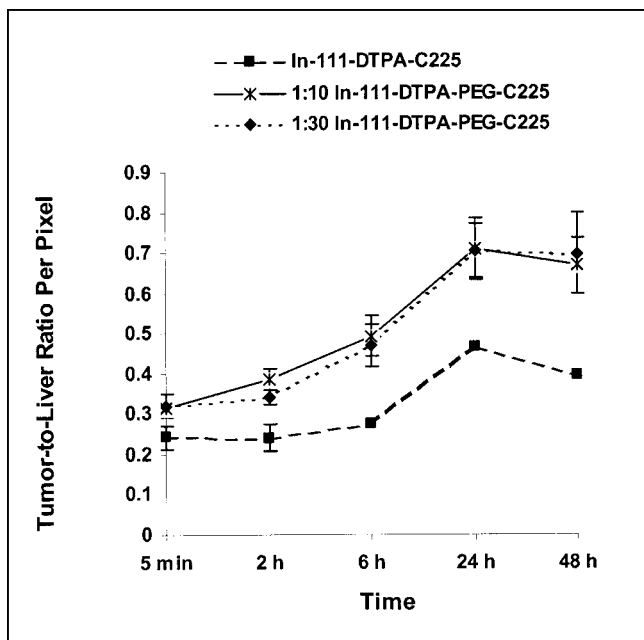


**FIGURE 4.** Quantification of tumor-to-liver ratios from sequential  $\gamma$ -images of  $^{111}\text{In}$ -labeled C225 conjugates. Data are expressed as ratios of tumor-to-liver radioactivity per pixel and presented as mean  $\pm$  SEM ( $n = 3$ ). Tumor-to-liver ratios for both PEG-modified C225 conjugates are significantly higher than ratio for C225 without PEG at each time point ( $P < 0.05$ ).

not shown). Although the quantification of EGFR by Western blot is not accurate, the assay allowed comparison of the intensities of the bands for the 3 cell lines and estimation of relative receptor expression.  $\gamma$ -Scintigrams of A431, MDA-MB-468, and MDA-MB-435 xenografts are presented in Figure 6. Both A431 and MDA-MB-468 tumors in the chest and hind limb sites showed substantial activity 24 h after injection of 1:30  $^{111}\text{In}$ -DTPA-PEG-C225. In contrast, less tumor activity was visualized in MDA-MB-435 tumors than in the other 2 tumor xenografts.

Dissection analysis performed 48 h after injection of 1:30  $^{111}\text{In}$ -DTPA-PEG-C225 showed the tumor-to-blood ratios for A431 and MDA-MB-468 xenografts were significantly higher than those for the MDA-MB-435 xenografts ( $P = 0.009$  for A431 tumors;  $P < 0.001$  for MDA-MB-468 tumors) (Fig. 7). Pretreatment with C225 20 h before injection of 1:30  $^{111}\text{In}$ -DTPA-PEG-C225 significantly reduced the tumor-to-blood ratios for A431 ( $P = 0.04$ ) and MDA-MB-468 ( $P < 0.001$ ) tumors but not for MDA-MB-435 tumors ( $P = 0.3$ ) (Fig. 7).

## DISCUSSION

The clinical application of many monoclonal antibodies in radioimmunodetection has been limited by significant liver uptake, which has made it difficult to visualize lesions inside or close to the liver. Our objective was to develop a labeling strategy for antibodies that will lead to a reduction in nonspecific interaction, increased tumor-to-liver ratio, and improved imaging properties. Therefore, we introduced the radiometal chelator DTPA to one end of a flexible, nontoxic polymer (PEG) and conjugated PEG to C225, an anti-EGFR antibody. Modification of the protein with PEG confers several advantageous and unique characteristics, including improved biocompatibility, increased circulation half-life, decreased immunogenicity, increased resistance to proteolysis, and enhanced solubility and stability (17). PEG modification also interferes with the recognition of foreign particles and proteins by the reticuloendothelial system and thus reduces the liver uptake (18,19). To avoid excessive manipulation of C225, we attached DTPA through the PEG linker instead of coupling DTPA and PEG sequentially to C225. Previous studies have established that PEG-modified C225 (i.e., DTPA-PEG-C225 conjugates) retained C225's biologic activity in binding to the EGFR in A431 cells and in inducing apoptosis in DiFi cells. More importantly, both in vitro competitive binding studies and pharmacokinetic

**TABLE 1**  
Distribution of 1:30  $^{111}\text{In}$ -DTPA-PEG-C225

Groups	Blood	Liver	Muscle	Tumor	Tumor-to-blood	Tumor-to-muscle
1:30 $^{111}\text{In}$ -DTPA-PEG-C225	1.40 $\pm$ 0.64	25.5 $\pm$ 2.0	0.69 $\pm$ 0.22	8.68 $\pm$ 1.78	7.04 $\pm$ 1.94	13.4 $\pm$ 3.89
$^{111}\text{In}$ -DTPA-C225	0.54 $\pm$ 0.24*	46.9 $\pm$ 2.5*	0.38 $\pm$ 0.08†	11.0 $\pm$ 1.0	22.3 $\pm$ 7.2*	29.4 $\pm$ 3.3*
C225 + PEGylated C225; 30-min	4.95 $\pm$ 0.61*	16.5 $\pm$ 4.25†	1.48 $\pm$ 0.22†	13.85 $\pm$ 1.38†	2.83 $\pm$ 0.49†	9.37 $\pm$ 0.58
C225 PEGylated C225; 20-h	2.93 $\pm$ 0.60†	10.5 $\pm$ 0.40*	0.73 $\pm$ 0.11	7.63 $\pm$ 1.96	2.59 $\pm$ 0.14†	10.4 $\pm$ 1.19

\* $P < 0.005$  compared with 1:30  $^{111}\text{In}$ -DTPA-PEG-C225 group.

† $P < 0.05$  compared with 1:30  $^{111}\text{In}$ -DTPA-PEG-C225 group.

Nude mice with EGFR-positive human A431 tumors were injected with 1:30  $^{111}\text{In}$ -DTPA-PEG-C225 or  $^{111}\text{In}$ -DTPA-C225. Additional 2 groups of mice were pretreated with native C225 30 min or 20 h before injection of 1:30  $^{111}\text{In}$ -DTPA-PEG-C225. Mice were dissected 48 h after radiotracer injection, and tissue samples were counted for radioactivity. Data are expressed as mean  $\pm$  SD of 3 mice per group (%ID/g).

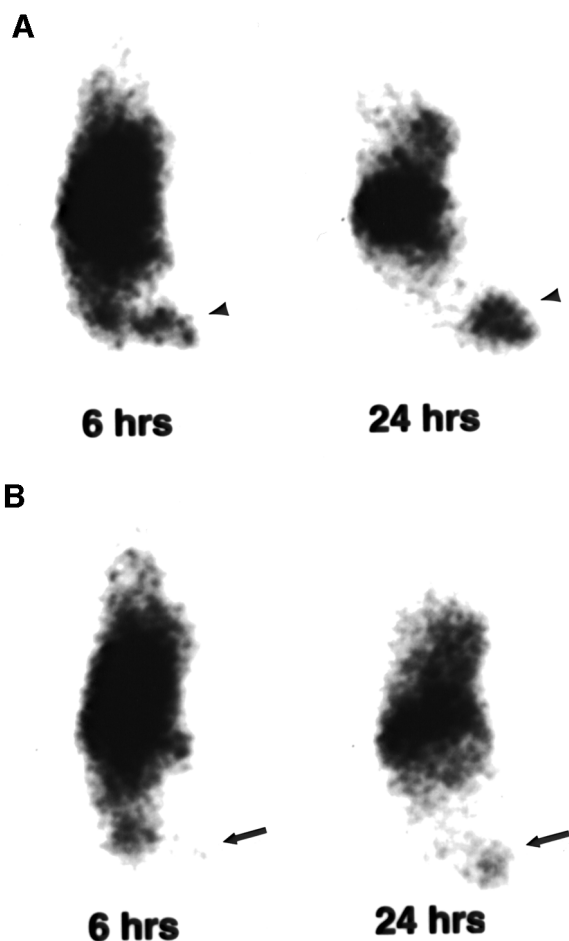


**FIGURE 5.** Representative  $\gamma$ -images of mice without (A) and with (B) C25 pretreatment 6 and 24 h after radiotracer injection. Mice with A431 tumors were injected with 1:30  $^{111}\text{In}$ -DTPA-PEG-C225 alone or 20 h after injection of unlabeled C225 at dose of 1 mg per mouse. Pairs of mice used in imaging study were matched for size of tumors. Tumors (arrowheads) in mouse injected with only 1:30  $^{111}\text{In}$ -DTPA-PEG-C225 are clearly visualized (A), whereas tumors (arrows) in mouse pretreated with C225 are hardly seen (B). Anterior views of mouse placed prone on camera's pinhole collimator, with head pointing to top.

studies showed that DTPA-PEG-C225 has lower nonspecific interaction with cells and tissues than DTPA-C225 (15).

EGFR-positive A431 cancer xenografts were imaged successfully using 1:10 DTPA-PEG-C225 or 1:30 DTPA-PEG-C225 labeled with  $^{111}\text{In}$  (Figs. 2 and 3). PEG modification significantly reduced liver uptake of C225, which was clearly visualized at later time points, that is, at 24 and 48 h after radiotracer injection (compare Fig. 1 with Figs. 2 and 3). The extent of reduction in liver activity was a function of the degree of PEG modification; 38% and 45% reductions were observed with 1:10 DTPA-PEG-C225 and 1:30 DTPA-PEG-C225, respectively. Modification with PEG had no effect (for 1:10 DTPA-PEG-C225) or only a mild

effect (for 1:30 DTPA-PEG-C225) on tumor uptake of  $^{111}\text{In}$ -DTPA-PEG-C225. As a result, tumors were better delineated with  $^{111}\text{In}$ -DTPA-PEG-C225 conjugates than with  $^{111}\text{In}$ -DTPA-C225. Observations made by visualization of images were supported by quantification from sequential scintigraphic images. Reduction of hepatic uptake of PEG-modified C225 was clearly indicated by the increased values of tumor-to-liver ratio per pixel for both 1:10 and 1:30 DTPA-PEG-C225 derivatives at each time point (Fig. 4). This increase was mainly a function of decreased liver uptake rather than increased tumor uptake, because modification with PEG molecules did not cause significant changes in tumor uptake of C225. These data indicated that, with appropriate control of the degree of substitution, PEG-modified C225 was a more effective tumor-targeting agent than directly labeled C225 for receptor imaging of cancer.

Quantitative ROI analysis showed that the radioactivity in tumors relative to the whole body increased with time and reached the maximum at 24 h for all 3 C225 radiotracers (data not given). The similarity in the kinetics of tumor uptake for PEG-modified C225 and C225 without PEG suggests that the retention of DTPA-PEG-C225 conjugates and DTPA-C225 in tumors is mediated by the same mechanism. To show that the tumor uptake of  $^{111}\text{In}$ -DTPA-PEG-C225 is indeed mediated through its binding to EGFR, we pretreated the A431 tumor-bearing mice with 100-fold excess of unlabeled C225 to block the receptors on cell surfaces. Reduced tumor radioactivity was clearly visualized at 6 h and 24 h after radiotracer injection in mice pretreated with C225 20 h before the injection of  $^{111}\text{In}$ -DTPA-PEG-C225 (Fig. 5). The observations made with  $\gamma$ -scintigrams were supported by dissection analysis performed 48 h after the injection of  $^{111}\text{In}$ -DTPA-PEG-C225. The tumor-to-blood ratios decreased 2.5–2.7 fold after pretreatment with C225 either 30 min or 20 h before the injection of  $^{111}\text{In}$ -DTPA-PEG-C225. Pretreatment with C225 also markedly reduced the liver uptake of  $^{111}\text{In}$ -DTPA-PEG-C225, probably as a result of blockage of nonspecific phagocytosis. The higher tumor uptake of  $^{111}\text{In}$ -DTPA-PEG-C225 observed when native C225 was injected 30 min before the radiotracer (Table 1) was most likely the result of its higher blood activity caused by the blockage of liver uptake and elimination. The high level of blood activity of the radiotracer conjugate permitted a greater proportion of the injected dose of the radiotracer to diffuse into the interstitial space and bind to receptors on the cancer cells. It is interesting to note that the 20-h blocking group had decreased uptake in the blood, liver, muscle, and tumor when compared with the 30-min blocking group (Table 1), suggesting that C225 preinjection may affect the clearance of PEGylated C225. Clearly, more studies are needed to clarify the role of C225 preinjection on the biodistribution properties of PEGylated C225.

$\gamma$ -Imaging studies with human tumor xenografts that express different levels of EGFR provide further support for the specific binding of PEG-modified C225 to the EGFR in

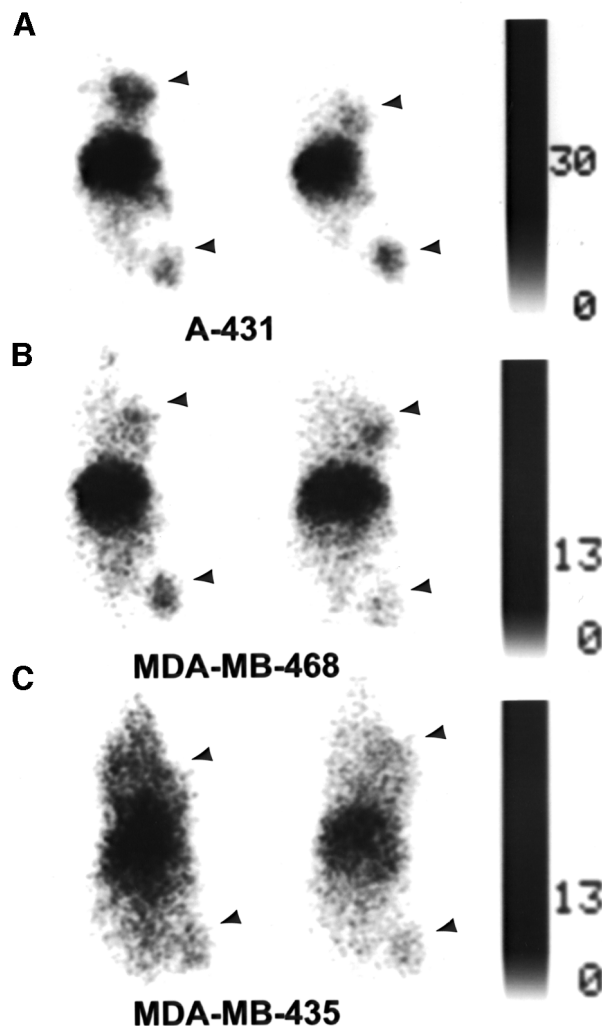


**FIGURE 6.**  $\gamma$ -Scintigrams of human tumor xenografts expressing different levels of EGFR. Mice with A431 (A), MDA-MB-468 (B), or MDA-MB-435 tumors (C) received 10  $\mu$ g per mouse of 1:30  $^{111}\text{In}$ -DTPA-PEG-C225 intravenously. Images were acquired 24 h after radioligand injection. A431 (A) and MDA-MB-468 tumors (B; arrowheads) are more readily visualized than MDA-MB-435 tumors (C; arrowheads). Anterior views of mice placed prone on camera's pinhole collimator, with heads pointing to top.

tumors. Tumors in A431 and MDA-MB-468 xenografts that express high levels of EGFR were clearly visualized on  $\gamma$ -images, whereas tumors in MDA-MB-435 xenografts with low levels of EGFR expression were not as readily seen (Fig. 6). In fact, the tumor-to-blood ratios of  $^{111}\text{In}$ -DTPA-PEG-C225 in A431 and MDA-MB-468 xenografts were about 3 fold higher than in MDA-MB-435 xenografts. The values were significantly reduced by pretreatment with C225 in mice with A431 and MDA-MB-468 tumors but not in mice with MDA-MB-435 tumors (Fig. 7). These results suggest that PEG-modified C225 retained its receptor-binding affinity in vivo and that its uptake in the tumor is mediated through EGFR.

The ability of  $^{111}\text{In}$ -DTPA-PEG-C225 to differentiate the level of EGFR expression in vivo suggests that this radioligand may be useful in characterizing the EGFR status of solid tumors. It is important to note that C225 does not react with mouse EGFR. Therefore, reduction in nonspecific liver uptake may not be sufficient to reduce liver radioactivity of PEGylated C225 in humans, where specific uptake of C225 in the liver by hepatic EGFR is expected. Divgi et al. (13) have shown that with  $^{111}\text{In}$ -DTPA-labeled C225, nearly all radioactivity was imaged in the liver if the C225 dose was <40 mg per patient. Improved tumor visualization was achieved only at higher doses of C225 when specific uptake is suppressed by saturating the hepatic EGFR (13). It is, therefore, possible to achieve further reduction in the liver uptake of PEGylated antibody by pretherapy with native antibody. Obviously, these points need to be addressed in a clinical setting.

In this study, C225 was used as a model compound. Whether PEGylation causes changes in potential immunogenicity has not been determined. Thus far, clinical experiences with C225 show little human antimouse antibody response with this antibody. Therefore, PEGylation may not

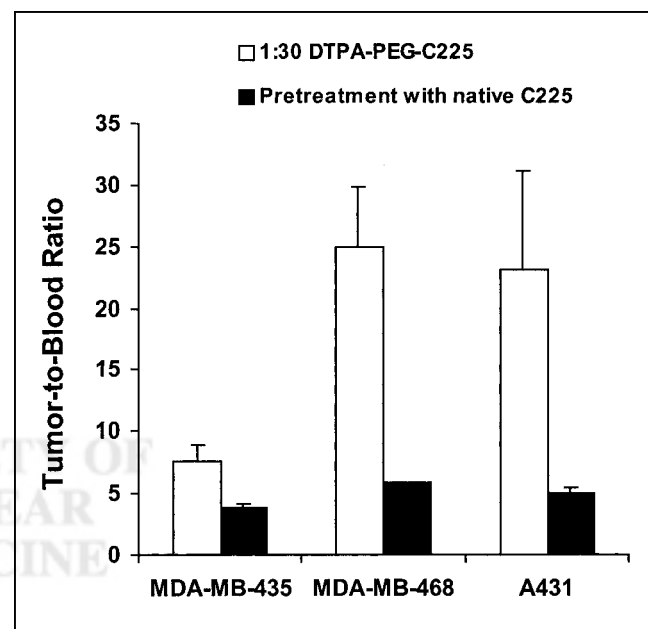


**FIGURE 7.** Tumor-to-blood ratios for mice bearing human A431, MDA-MB-468, or MDA-MB-435 xenografts with or without C225 pretreatment. Mice were injected intravenously with 10  $\mu$ g per mouse of 1:30  $^{111}\text{In}$ -DTPA-PEG-C225 alone or 20 h after pretreatment with native C225 and killed 48 h later; tissues were removed for radioactivity quantification. Data, expressed as ratios of ID/g in tumor to ID/g in blood, are presented as mean  $\pm$  SEM ( $n = 3$ ). Tumor-to-blood ratios for A431 and MDA-MB-468 tumors are significantly higher ( $P = 0.009$  and  $P < 0.001$ , respectively) than ratio for MDA-MB-435 tumors. Pretreatment with C225 resulted in significant decreases of tumor-to-blood ratios for A431 and MDA-MB-468 tumors ( $P = 0.04$  and  $P < 0.001$ , respectively) but not for MDA-MB-435 tumors ( $P = 0.3$ ).

benefit C225 with regard to reduction of immunogenicity. However, PEGylation should have a significant impact on immunogenicity of other proteins or nonhumanized antibodies intended for imaging purposes.

## CONCLUSION

The results of this study show that a labeling technique using the PEG polymer with the radiometal chelator DTPA attached to one end of the polymer chain can lead to reduced nonspecific interaction and reduced liver uptake.  $\gamma$ -Imaging and distribution studies with a monoclonal antibody directed against EGFR indicate that the tumor uptake of a PEG-modified antibody was mediated through the receptors. The level of tumor localization in vivo is different in tumors with a different amount of receptors, suggesting that noninvasive characterization of receptor expression is possible. Clinical studies of  $^{111}\text{In}$ -DTPA-PEG-C225 are needed to clarify the effect of PEGylation on the specific liver uptake of the C225 antibody.

## ACKNOWLEDGMENTS

The authors thank Scott Miller for assistance with  $\gamma$ -scintigraphic studies and Kathryn Hale for editorial assistance. Human breast adenocarcinoma cell lines MDA-MB-468, MDA-MB-435, and human vulvar squamous carcinoma cell line A431 were obtained from Dr. Zhen Fan. This study was supported in part by the John S. Dunn Foundation.

## REFERENCES

1. Modjahedi H, Dean C. The receptor for EGF and its ligands: expression, prognostic value and target for therapy in cancer (review). *Int J Oncol*. 1994;4:277–296.
2. Ethier SP. Growth factor synthesis and human breast cancer progression. *J Natl Cancer Inst*. 1995;87:964–973.
3. Wataru Y, Hiromichi S, Jotaro H, et al. Expression of epidermal growth factor

receptor in human gastric and colonic carcinomas. *Cancer Res*. 1988;48:137–141.

4. Mendelsohn J. Epidermal growth factor receptor inhibition by a monoclonal antibody as anticancer therapy. *Clin Cancer Res*. 1997;3:2703–2707.
5. Fan Z, Masui H, Altas I, Mendelsohn J. Blockage of epidermal growth factor receptor function by bivalent and monovalent fragments of 225 anti-epidermal growth factor receptor monoclonal antibodies. *Cancer Res*. 1993;53:4322–4328.
6. Ennis BW, Valverius EM, Bates SE, et al. Anti-epidermal growth factor receptor antibodies inhibit the autocrine-stimulated growth of MDA-468 human breast cancer cells. *Mol Endocrinol*. 1989;3:1830–1838.
7. Wu X, Fan Z, Masui H, et al. Apoptosis induced by an anti-epidermal growth factor receptor monoclonal antibody in a human colorectal carcinoma cell line and its delay by insulin. *J Clin Invest*. 1995;95:1897–1905.
8. Mendelsohn J, Masui H, Goldenberg A. Anti-epidermal growth factor receptor monoclonal antibodies may inhibit A431 tumor cell proliferation by blocking autocrine pathway. *Trans Assoc Am Physicians*. 1987;100:173–178.
9. Masui H, Kawamoto T, Sato JD, et al. Growth inhibition of human tumor cells in athymic mice by anti-epidermal growth factor receptor monoclonal antibodies. *Cancer Res*. 1984;44:1002–1007.
10. Fan Z, Baselga J, Masui H, Mendelsohn J. Antitumor effect of anti-epidermal growth factor receptor monoclonal antibodies plus cis-diamminedichloroplatinum on well established A431 cell xenografts. *Cancer Res*. 1993;53:4637–4642.
11. Baselga J, Pfister D, Cooper MR, et al. Phase I studies of anti-epidermal growth factor receptor chimeric antibody C225 alone and in combination with cisplatin. *J Clin Oncol*. 2000;18:904–914.
12. Goldenberg A, Masui H, Divgi C, et al. Imaging of human tumor xenografts with an indium-111-labeled anti-epidermal growth factor receptor monoclonal antibody. *J Natl Cancer Inst*. 1989;82:1616–1625.
13. Divgi CR, Welt S, Kris M, et al. Phase I and imaging trial of indium-111-labeled anti-epidermal growth factor receptor monoclonal antibody 225 in patients with squamous cell lung carcinoma. *J Natl Cancer Inst*. 1991;83:97–104.
14. Reilly RM, Kiarash R, Sandhu J, et al. A comparison of EGF and mAb 528 labeled with  $^{111}\text{In}$  for imaging human breast cancer. *J Nucl Med*. 2000;41:903–911.
15. Wen XX, Wu QP, Lu Y, et al. Poly(ethylene glycol)-conjugated anti-EGF receptor antibody C225 with radiometal chelator attached to the termini of polymer chains. *Bioconjug Chem*. 2001;12:545–553.
16. Hnatowich DJ, Layne WW, Childs RL, et al. Radioactive labeling of antibody: a simple and efficient method. *Science*. 1983;220:613–615.
17. Fuertges F, Abuchowski A. The clinical efficacy of poly(ethylene glycol)-modified proteins. *J Controlled Release*. 1990;11:139–148.
18. Takashina K, Kitamura K, Yamaguchi T, et al. Comparative pharmacokinetic properties of murine monoclonal antibody A7 modified with neocarzinostatin, dextran and polyethylene glycol. *Jpn J Cancer Res*. 1991;82:1145–1150.
19. Shimada K, Kamps J, Regts J, et al. Biodistribution of liposomes containing synthetic galactose-terminated diacylglycerol-poly(ethyleneglycol)s. *Biochim Biophys Acta*. 1997;1326:329–341.

